energies

Article

Coordination Mechanism Between Electric Vehicles and Air Conditioning Loads Based on Price Guidance

Dan Wu [1], Danting Zhong [2,*] and Lili Li [2]

[1] State Grid Shanghai Municipal Electric Power Company, Shanghai 200437, China; wooden_sh@163.com
[2] Sichuan Energy Internet Research Institute, Tsinghua University, Chengdu 610042, China; lilili@tsinghua-eiri.org
* Correspondence: zhongdanting@tsinghua-eiri.org

Abstract

Under China's dual carbon goals, the surging summer demand for air conditioning (AC) has widen the power grid's peak-to-valley difference, posing challenges to conventional supply-side solutions. To address this issue, effective demand-side coordination is essential. However, existing demand response schemes typically optimize single resources in isolation and overlook the dynamic evolution of user participation. This study proposes a price-guided coordination mechanism integrating vehicle-to-grid (V2G) and AC loads to establish a closed-loop value chain among the grid, aggregators, and users. A bi-level optimization framework is developed to balance the interests of these stakeholders. The model incorporates a V2G discharging willingness component that considers user psychology and battery degradation, as well as an AC response model reflecting thermal comfort. Simulation results demonstrate that the proposed mechanism effectively mitigates peak loads and narrows the peak-to-valley difference while enhancing off-peak electricity consumption. It accommodates the spatiotemporal and user-type heterogeneity of response behaviors, yielding notable economic gains for all participants. This research validates a comprehensive strategy for improving grid flexibility, protecting stakeholder interests, and optimizing user engagement, offering both theoretical insight and practical guidance for diversified resource integration.

Keywords: demand response; V2G; air conditioning; coordination; bi-level optimization; price mechanism

check for updates

Academic Editor: Jay Zarnikau

Received: 15 October 2025
Revised: 10 November 2025
Accepted: 13 November 2025
Published: 14 November 2025

Citation: Wu, D.; Zhong, D.; Li, L. Coordination Mechanism Between Electric Vehicles and Air Conditioning Loads Based on Price Guidance. *Energies* **2025**, *18*, 5984. https://doi.org/10.3390/en18225984

Copyright: © 2025 by the authors. Licensee MDPI, Basel, Switzerland. This article is an open access article distributed under the terms and conditions of the Creative Commons Attribution (CC BY) license (https://creativecommons.org/licenses/by/4.0/).

1. Introduction

The ongoing urbanization process in China has led to substantial growth in air conditioning (AC) loads during summer and winter, making them major contributors to peak electricity demand. Empirical studies demonstrate that in certain regions, AC loads account for over 40% of total electricity consumption during summer peak hours [1,2]. Traditional approaches to maintaining grid stability primarily rely on expanding generation capacity, typically through the installation of additional gas turbines. However, this method presents several limitations, including high capital investment, long construction periods, low annual utilization rates [3], and limited economic viability. Under China's dual carbon targets, the development of conventional thermal power generation, particularly coal-fired power plants, faces increasing restrictions. Statistical evidence indicates a consistent decline in the proportion of thermal power within the installed capacity mix [4,5], prompting system operators to explore more flexible and cost-effective regulatory alternatives. As a result,

leveraging demand-side flexibility for adaptive peak load management has become a key research focus in the field of power system optimization.

The electric vehicle (EV) market has experienced rapid and sustained growth in recent years. EVs and AC loads exhibit a highly correlated spatiotemporal distribution across various application scenarios, such as commercial buildings, campuses, and residential communities, where both can be categorized as destination-oriented energy resources [6,7]. Notably, vehicle-to-grid (V2G) technology effectively harnesses the energy storage potential of EVs during parking periods, offering distinct advantages including minimal spatial requirements, significant regulation capacity, and low marginal costs. These characteristics establish a technically feasible and economically viable pathway for coordination between heterogeneous load types.

Price-based mechanisms constitute a fundamental approach for engaging consumers in demand response programs and have demonstrated significant potential in motivating participation from distributed resources such as V2G and AC users. Well-designed pricing schemes, including time-of-use tariffs, real-time pricing, and direct subsidies, can effectively shape user charging and discharging behaviors [8–10]. However, most existing studies adopt a single-stakeholder perspective, focusing exclusively on grid operational requirements [11], aggregator profit [12], or user economic and comfort preferences [13]. Such an isolated focus prevents the comprehensive alignment of interests among all stakeholders. Although a number of studies have attempted to integrate the objectives of grid operators, aggregators, and end-users, for instance, by minimizing peak-valley differences while improving participation rates [14], optimizing net power exchange and carbon emissions in distributed energy systems while reducing battery degradation costs [15], or balancing aggregator revenues with user electricity costs [16]. The predominant research emphasis remains on the response characteristics of individual resource types, particularly AC loads. This narrow scope tends to overlook both the spatial–temporal coupling effects and the coordination among multiple flexible resources. Demand response mechanisms designed for coordinated operation of V2G and AC loads are still in early stages of development, lacking well-developed market architectures and mature pricing mechanisms for multi-resource coordination. In particular, there is a scarcity of in-depth research on integrated strategies that simultaneously incentivize both resource types while aligning the divergent interests of various stakeholders. This gap continues to hinder the realization of operational synergies and the full exploitation of demand-side flexibility in modern power systems.

The decision-making process for V2G and AC users regarding discharging behavior or load adjustment is inherently complex and influenced by multiple interrelated factors. Key determinants include incentive levels, psychological preferences, and battery degradation costs [17,18]. For AC loads, variables such as household income, thermal comfort requirements, and user demographic characteristics significantly affect price response, exhibiting pronounced user heterogeneity [19]. In the case of EVs, battery degradation costs [20] and travel demand [21] constitute crucial determinants influencing user participation in discharging activities. Although existing studies have attempted to develop user response models, most retain oversimplified models, typically employing price or single cost components as core variables [22], while overlooking the combined influence of psychological, behavioral, and technical dimensions. Consequently, these models fail to accurately capture the intrinsic complexity of actual user decision-making processes. Therefore, developing sophisticated, multi-dimensional behavioral response models that incorporate user heterogeneity constitutes a crucial research direction for enhancing the coordination between V2G and AC loads.

Addressing these research limitations, this paper first systematically examines both qualitative and quantitative aspects of the necessity and feasibility of coordinating des-

tination AC and V2G loads from the perspectives of grid regulation requirements and resource spatiotemporal characteristics. Building upon this foundation and targeting the coordination requirements of AC and V2G resources, a dynamic price-guided coordination mechanism is proposed to establish a closed-loop value transfer framework connecting the grid, load aggregators, and end-users. Within this framework, a bi-level optimization game model is developed to facilitate the coordination of V2G and AC loads. This model incorporates utility functions of multiple stakeholders, including the grid, load aggregators, and consumers. Simultaneously, it introduces a V2G discharging willingness model that captures user price elasticity, behavioral psychology, and battery degradation costs. In parallel, an AC response willingness model is formulated to account for users' thermal comfort preferences, thereby enabling a more refined representation of heterogeneous user response behaviors. Finally, case studies are conducted to validate the effectiveness of the proposed mechanism. The results demonstrate its superior performance in enhancing social welfare, ensuring individual rationality, improving user experience, and strengthening demand response efficiency. These findings provide both a theoretical foundation and methodological guidance for coordination strategies applicable to other heterogeneous demand-side resources.

2. Problem Definition and Motivation

2.1. Characteristics of EV and AC Loads

With the continuing advancement of urbanization, AC loads and destination charging loads exhibit a peak-on-peak phenomenon, thereby exacerbating stress on the power grid. AC loads constitute a major contributor to peak electricity demand in both summer and winter seasons. These loads are characterized by high temperature sensitivity and low demand elasticity, primarily owing to their strong association with human thermal comfort requirements. Empirical studies indicate that grid load rises sharply with increasing ambient temperatures, particularly when outdoor temperatures climb from 33.3 °C to 44.4 °C [23]. Data from Shanghai show that cooling loads in residential and commercial buildings account for more than 30% of the total load during peak hours in both summer and winter [24]. The comparative relationship between typical daily grid load and AC load is illustrated in Figure 1.

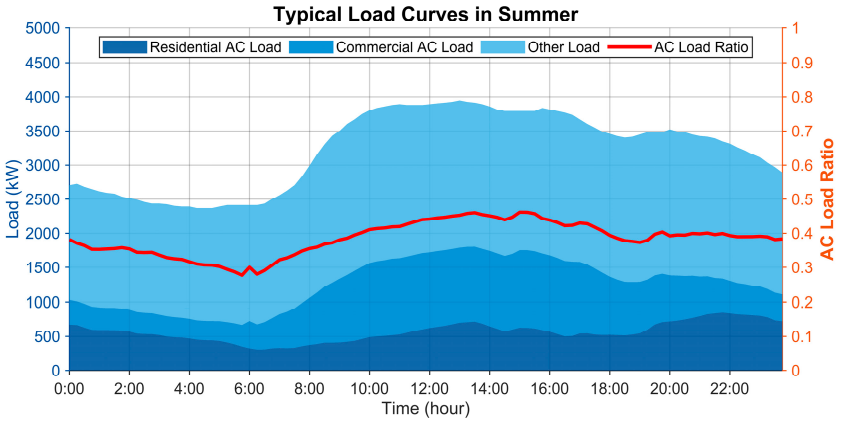


Figure 1. Comparison of typical daily grid load and AC load curves in Shanghai in summer.

Regarding charging loads, destination charging constitutes a critical component of EV charging load, characterized by both a large user base and considerable load magnitude. Destination charging refers to charging activities conducted by EV owners at locations where people spend extended periods of time, such as offices, commercial buildings, and residential communities [25]. Empirical data from Shanghai indicate that on typical

working days, destination charging in residential and office areas accounts for up to 70% of the total public charging load. The temporal variation in the proportion of destination charging throughout the day is illustrated in Figure 2.

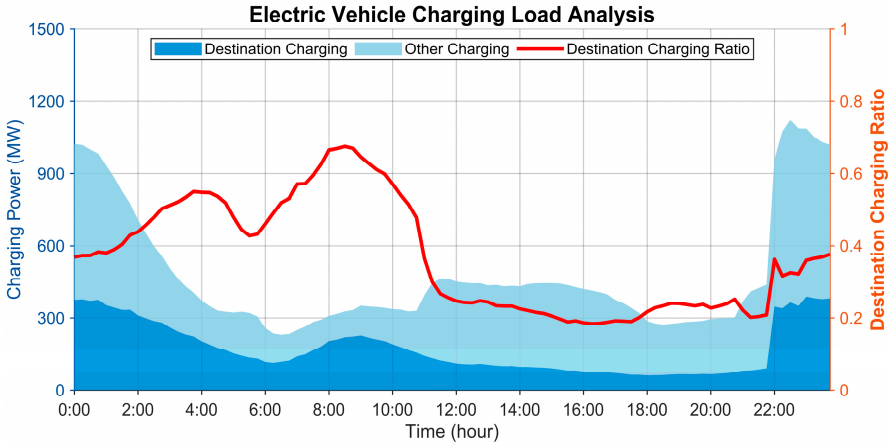


Figure 2. Ratio of destination charging load to total charging load.

The independent regulation of AC loads faces several inherent limitations, including unidirectional adjustment capability, the sacrifice of users' comfort, and restricted flexibility. Current AC load management strategies primarily rely on adjusting operational parameters or improving equipment efficiency. Although such measures can achieve peak load shaving, they fail to enable valley filling and thus cannot promote the absorption of renewable energy, thereby constraining AC flexibility. Moreover, prolonged limited power operation frequently leads to user complaints due to degraded indoor comfort levels [26], which further diminishes the adjustable potential.

EVs have now reached large-scale deployment, with V2G technology emerging as an innovative solution to mitigate supply challenges posed by AC loads and enhance grid operational flexibility. The principal advantages of the V2G approach are twofold. First, EVs in destination scenarios exhibit strong spatiotemporal correlation with AC loads. Specifically, residential users typically activate both household AC systems and V2G equipment upon returning home in the evenings, whereas commercial facilities operate central AC systems while simultaneously offering charging and discharging services for employees' vehicles during the daytime. By implementing coordinated load management across these scenarios and leveraging V2G discharge capabilities, significant reductions in grid peak demand can be achieved, ultimately achieving comprehensive peak shaving and valley filling goals. The spatiotemporal distribution of user travel and charging behavior is illustrated in Figure 3.

Second, compared with conventional AC load regulation methods such as temperature setpoint optimization, V2G technology offers distinct advantages, including bidirectional regulation capacity encompassing both peak shaving and valley filling, prolonged vehicle parking durations, and considerable economic benefits. These characteristics establish V2G as a high-quality, cost-effective flexibility resource for the power grid. A detailed comparative analysis of these attributes is summarized in Table 1.

2.2. Spatiotemporal Coupling Characteristics

Both AC and V2G systems, as destination-based resources, share strong spatial and temporal correlations and complement the temporal patterns of charging loads. This inherent spatiotemporal coupling provides the physical foundation for leveraging V2G to shave AC peak loads.

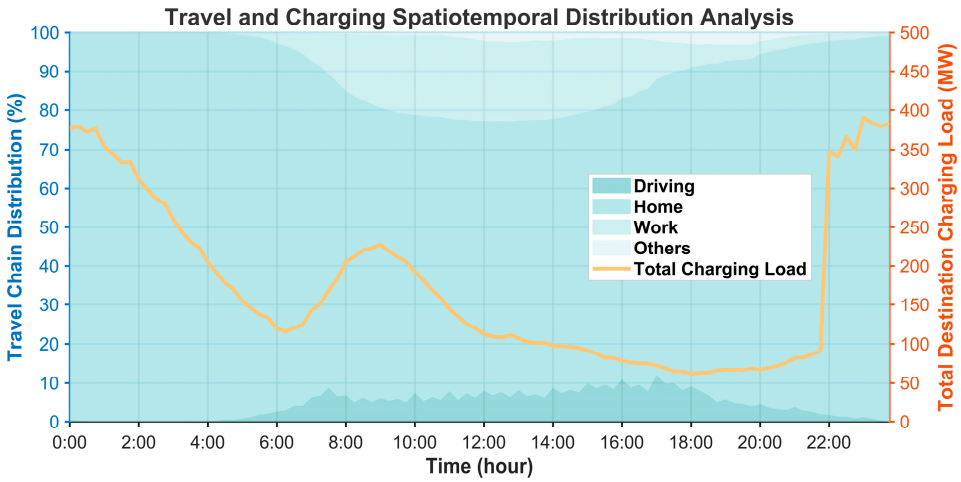


Figure 3. Spatiotemporal distribution of user travel and charging behavior.

Table 1. Comparison Between V2G and AC Loads.

Regulation Method	Peak Shaving	Valley Filling	Implementation Complexity	User Experience
AC	√ (limited)	×	Low	Sacrificing comfort
V2G	√	√	Low	Minimal user awareness, negligible impact

Note: The symbols "√" and "×" indicate the presence or absence of a specific capability, respectively.

To quantitatively assess the spatiotemporal coupling characteristics between AC loads and EVs, this study introduces a set of evaluation indicators for measuring the coupling of mobile energy resources. Specifically, a normalized similarity framework is proposed to define two key metrics: the spatiotemporal coupling between AC load and discharging load, and that between AC load and charging load. These metrics characterize the correlation between the two types of resource across both temporal and spatial dimensions, satisfying the following equations.

$$\gamma_{\text{dis}} = 1 - |P^*_{\text{act}} - N^*_{\text{cart}}| \tag{1}$$

$$\gamma_{\text{ch}} = 1 - |P^*_{\text{act}} - P^*_{\text{EV}t}| \tag{2}$$

where γ_{dis} and γ_{ch} represent the spatiotemporal coupling between AC load and discharging load, and that between AC load and charging load, respectively; P^*_{act} denotes the normalized AC load at time t; N^*_{cart} indicates the normalized value of parked vehicles at time t; and $P^*_{\text{EV}t}$ represents the normalized charging load at time t. A higher γ_{dis} indicates a greater degree of spatiotemporal overlap between vehicle parking rates and AC loads, implying a stronger potential for V2G discharging to regulate AC loads. Conversely, a lower γ_{ch} reflects better temporal coordination between AC loads and charging loads, reducing the risk of peak-on-peak load.

Normalized values are obtained using max-min normalization, which scales each variable to the unit interval [0, 1]. For any variable V, the normalized value V^*_t is calculated as follows.

$$V^*_t = \frac{V_t - \min(V_t)}{\max(V_t) - \min(V_t)} \tag{3}$$

where V_t represents the original value of the variable at time t, $\max(V_t)$ and $\min(V_t)$ denote the maximum and minimum value of variable V, respectively.

Using data from Shanghai as a case study, the proposed evaluation indicators were applied to quantify spatiotemporal coupling characteristics across different regions. The

resulting heatmap, which illustrates the spatiotemporal coupling between residential and office areas, is shown in Figure 4.

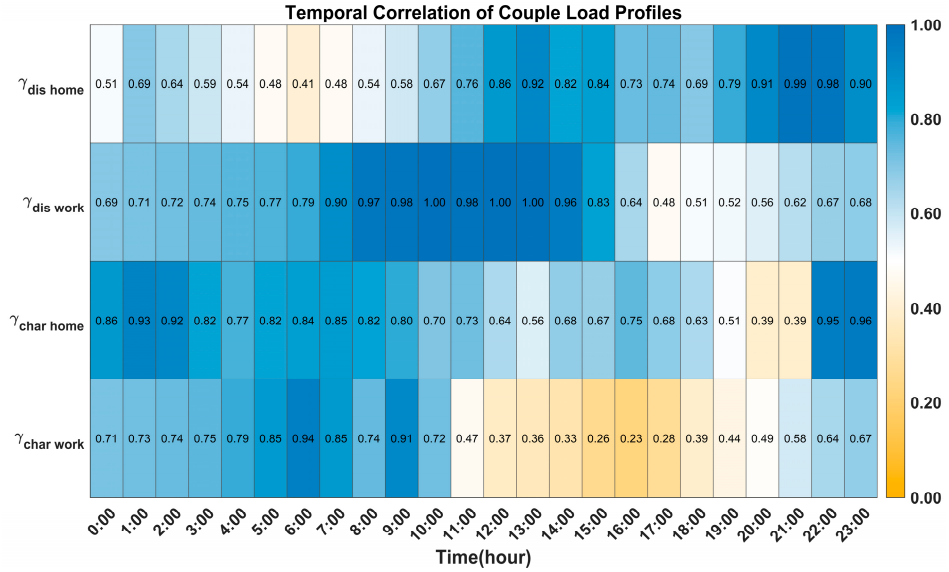


Figure 4. Spatiotemporal coupling heatmap of user traffic and charging behaviors in residential and office areas.

The results indicate that, from the perspective of V2G discharge potential, γ_{dis} for both residential and office areas, generally exceed 0.5. Specifically, γ_{dis} in office areas exceeds 0.7 during the daytime AC load peak hours (08:00–16:00), whereas γ_{dis} in residential areas, demonstrate surpasses 0.7 during the evening AC load peak hours (19:00–24:00). These findings reveal a strong spatiotemporal alignment between V2G discharge capability and AC loads during these periods, suggesting significant peak shaving potential.

From the perspective of charging load coordination, γ_{ch} in residential areas remains below 0.5 during daytime hours (08:00–18:00), indicating effective temporal load shifting. However, these values rise to above 0.6 during nighttime hours (22:00–24:00), suggesting potential peak-on-peak risk caused by concurrent AC operation and EV charging. Similarly, γ_{ch} in office areas exceeds 0.6 during morning commute hours (08:00–10:00) on weekdays, implying the necessity of charging load peak-shifting to mitigate load superposition during this period.

In summary, the analysis reveals substantial spatiotemporal overlap between EV parking behaviors and AC loads. Without appropriate coordination, such an overlap could intensify grid stress during peak hours. Therefore, there is an urgent need to develop an efficient and cost-effective coordination mechanism between AC loads and charging loads.

3. Design of a Price-Guided Coordination Mechanism

3.1. Principles of Mechanism Design

To address the coordination challenges identified in Section 2, a price-guided coordination mechanism for integrating V2G and AC loads is proposed in this section. The core of effective coordination lies in the formulation of a dynamic incentive pricing mechanism that is scientifically grounded, reasonable, and sustainable. Such a mechanism should not only encourage active user participation but also balance the interests of all stakeholders, including the grid, aggregators, and users. The proposed coordination mechanism is built upon three core principles, namely economic efficiency, consumer protection, and system sustainability [27]. These mechanisms must balance efficiency with equity while ensuring long-term operational sustainability.

A. Economic Efficiency Principle: This principle forms the core of electricity pricing design and aims to maximize total social welfare. The value created through V2G and AC load coordination originates from the collective contributions of multiple stakeholders. Therefore, total social welfare should equal the sum of net benefits across all participants, while ensuring that no individual participant incurs losses. This objective can be achieved through the construction and solution of optimization models.

B. Consumer Protection Principle: Serving as the cornerstone for maintaining user participation and trust, this principle requires transparency and accessibility in the determination of discharge electricity prices, real-time pricing, and historical data. Furthermore, users who contribute equivalent value should receive equal incentives, thereby preventing price discrimination and promoting both transparency and fairness in the pricing process.

C. System Sustainability Principle: This principle emphasizes the long-term financial viability of the V2G model, particularly in relation to cost recovery mechanisms for discharge pricing. This paper proposes that the system benefits arising from V2G discharge, such as deferred investment in peak power generation capacity, should be recovered by applying critical peak prices to non-V2G end-users during peak hours. This approach establishes a beneficiary-pays virtuous cycle, prevents cross-subsidization through the socialization of costs, and ensures the sustainable development of V2G.

3.2. Closed-Loop Value Transfer Framework

To achieve efficient coordination between V2G and AC loads on the demand side, this section establishes a closed-loop value transfer framework characterized by value-driven incentives, price-guided coordination, and mutual beneficial outcomes for all stakeholders, as illustrated in Figure 5. Centered on dynamic incentive pricing as the signal, this framework integrates the entire value chain from the grid to aggregators and finally to end-users. The enhanced benefits are ultimately fed back into the power grid, forming a closed loop that ensures the sustainability of the model.

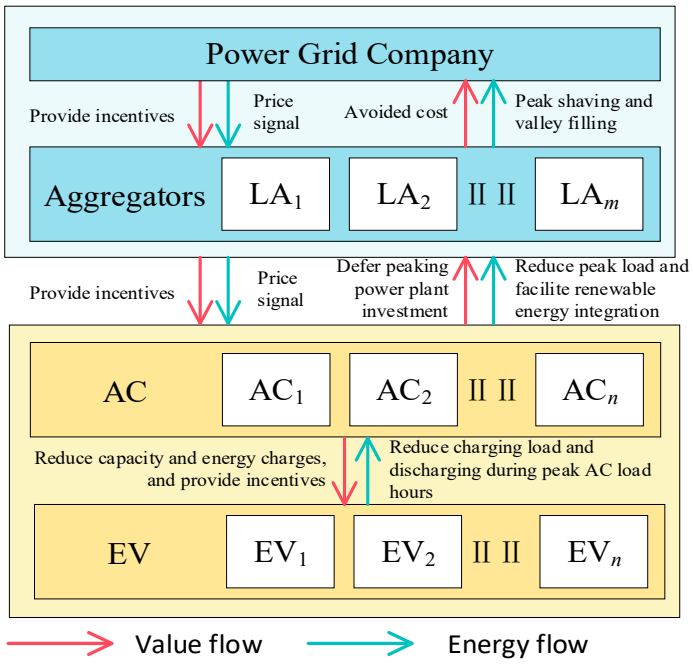


Figure 5. Closed-loop value transfer framework among grid company, aggregators, and users.

The primary stakeholders in demand-side resource coordination encompass the grid company, aggregators, and end-users. The respective roles and revenue streams of each party are outlined below.

A. Grid Company: As the system operator, the grid company acts as both the initiator of demand and the ultimate beneficiary of value generated through demand-side coordination. Its key objectives involve ensuring system reliability, reducing overall operating costs, and deferring grid infrastructure investments. By procuring flexibility services from aggregators, it circumvents the need to dispatch insufficient high-cost generators, thereby yielding significant economic gains from deferred capital expenditures and enhanced operational efficiency. The payments made for these services are substantially lower than the costs of conventional alternatives, resulting in positive net benefits.

B. Aggregators: Serving as pivotal intermediaries that link the grid with distributed end-users, aggregators pool dispersed V2G and AC resources and develop optimal scheduling strategies in line with grid demand. Through effective resource aggregation and coordination, they deliver high-quality demand response services at costs below electricity market prices, earning margin-based profits. Their main expenditures consist of incentive payments to end-users and operational platform costs, while their revenue originates from electricity market settlements with the grid company.

C. End-Users: Comprising EV owners and AC users, end-users represent the ultimate providers of flexibility. By responding to dynamic price signals from aggregators and adjusting their charging, discharging, cooling, or heating behaviors, they receive financial compensation. For EV users, discharging during peak hours must generate sufficient revenue to offset battery degradation costs and any loss of convenience. For AC users, moderately relaxing indoor temperature setpoints during high-temperature peak hours yields energy-saving incentives or direct payments, which should compensate for the temporary sacrifice in thermal comfort.

Within the closed-loop value chain involving the grid, aggregators, and users, the grid functions as the upper-level decision-maker. With objectives focused on maximizing social welfare, minimizing peak-to-valley load differences, and optimizing off-peak consumption, it formulates optimal demand response incentive curves and transmits corresponding price signals to lower-level decision-makers (i.e., aggregators). Aggregators, in turn, optimize for both their own net benefits and those of end-users, jointly determining optimal charging and discharging strategies while accounting for user responsiveness. The resulting discharge power then feeds back into the upper-level optimization, directly influencing the upper objective and ensuring iterative coordination.

4. Bi-Level Optimization Model of the Proposed Mechanism

4.1. Bi-Level Optimization Framework

To quantitatively implement the proposed mechanism, a bi-level optimization model is developed. The upper level represents the grid company's objective of maximizing total social welfare and the proportion of off-peak electricity consumption while minimizing the peak-to-valley load ratio. The lower level captures the aggregators' benefit-maximization behavior and user-side responses under price incentives. This bi-level game-theoretic optimization structure is illustrated in Figure 6.

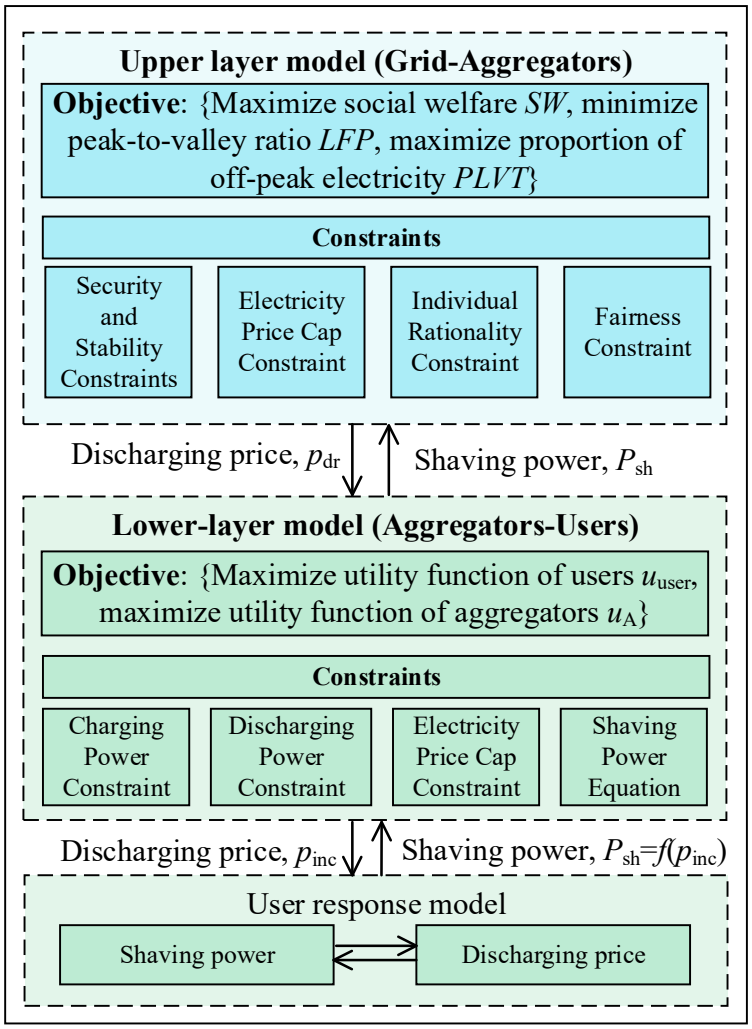


Figure 6. Bi-level optimization model framework.

4.2. Upper-Level Grid Optimization Model

4.2.1. Objective Function of Upper-Level Model

The primary objective of the upper level is to maximize the total social net welfare, defined as the sum of the net benefits for the grid company, aggregators, and all users, while simultaneously minimizing the peak-to-valley load difference and maximizing the proportion of off-peak electricity. To reconcile the non-commensurate nature of these objectives, a max-min normalization procedure is implemented. The objective function is expressed as follows.

$$F_{up} = \min[-f_1 SW - f_2/LFP - f_3 PLVT] \tag{4}$$

$$f_1 + f_2 + f_3 = 1 \tag{5}$$

where f_1, f_2, and f_3 represent the corresponding weighting coefficients, and *SW*, *LFP*, and *PLVT* denote the social welfare, peak-to-valley ratio, and proportion of off-peak electricity, respectively. The weighting coefficients f_1, f_2, and f_3 are systematically derived using the Analytic Hierarchy Process (AHP), which determines the final weights through eigenvector calculation.

A. Social Welfare

The social welfare is determined by the utility functions of the grid company, aggregators, and users, satisfying the following equation.

$$SW = u_{\mathrm{g}} + \sum_{i=1}^{N_{\mathrm{agg}}} u_{\mathrm{A},i} + \sum_{i=1}^{N_{\mathrm{user}}} u_{\mathrm{user},i} \tag{6}$$

where N_{agg} and N_{user} represent the number of aggregators and users, respectively; u_{g} is the utility function of the grid company; $u_{\mathrm{A},i}$ and $u_{\mathrm{user},i}$ represent the utility functions of the i-th aggregator and user, respectively.

(a) Utility Function of Grid Company

The utility function of the grid company is determined by the avoided costs resulting from peak shaving and valley filling, offset by the incentive payments for demand response, which can be expressed as follows.

$$u_g = ACC_{\mathrm{dr}} - \sum_{t \in T_{\mathrm{de}}} P_{\mathrm{sh},t,i} \Delta t p_{\mathrm{dr},t} \tag{7}$$

where ACC_{dr} represents the avoided cost due to load reduction, which is related to the total response electricity; $p_{\mathrm{dr},t}$ denotes the discharge price paid by the grid company to aggregators during time period t; $P_{\mathrm{sh},t,i}$ represents the total peak-shaving power from V2G users and AC users associated with the i-th aggregator during time period t; T_{de} indicates the demand response period; and Δt is the time interval.

(b) Aggregator Utility Function

The utility function of an aggregator reflects the response subsidies received from the grid company, the incentive payments provided to users, and the costs associated with V2G equipment investment and operation and maintenance (O&M). The utility function for the i-th aggregator satisfies the following equations.

$$u_{\mathrm{A},i} = -C_{\mathrm{V2G},i} + \sum_{y=1}^{n} \frac{R_{\mathrm{net},i,y}}{(1+IRR)^y} \tag{8}$$

$$R_{\mathrm{net},i,y} = -OM_{\mathrm{V2G},i,y} + \sum_{t \in T_{\mathrm{de}}} P_{\mathrm{sh},t,i,y} \Delta t (p_{\mathrm{dr},t} - p_{\mathrm{inc},t}) + CC_{\mathrm{save},i,y} \tag{9}$$

$$CC_{\mathrm{save},i,y} = \sum_{m=1}^{M} \Delta P_{\mathrm{C},m,i,y} p_{\mathrm{Ca},m} \tag{10}$$

where $R_{\mathrm{net},i,y}$ represents the annual net revenue in year y; C_{V2G} and OM_{V2G} represent the initial investment and annual O&M cost of V2G equipment, respectively; CC_{save} denotes annual savings from reduced capacity charges of the aggregator; $p_{\mathrm{inc},t}$ represents the discharge electricity price paid by the aggregator to users during time period t; n denotes the investment cycle in years; IRR indicates the internal rate of return; $\Delta P_{\mathrm{C},m,i,y}$ represents the reduction in user electricity capacity in month m of year y; M indicates the number of months; subscript i, y and m denotes the i-th aggregator, y-th year, and m-th month, respectively.

(c) Individual User Utility Function

The utility function of an individual user primarily depends on the incentives received for participating in discharge activities and the cost of charging during off-peak hours, satisfying the following equation.

$$u_{\text{user},i} = \sum_{y=1}^{n} \frac{\sum\limits_{t \in T_{\text{de}}} \left(P_{\text{sh},t,i,y} p_{\text{inc},t,i} - P_{\text{dis},t,i,y} p_{\text{ch,valley}} \right) \Delta t}{(1 + IRR)^y} \tag{11}$$

where $P_{\text{dis},t}$ represents the discharging power of V2G users during time period t, and $p_{\text{ch,valley}}$ denotes the charging electricity price during off-peak hours.

B. Peak-to-Valley Ratio

$$LFP = \frac{P_{\text{peak}}}{P_{\text{valley}}} \tag{12}$$

where P_{peak} and P_{valley} represent the maximum and minimum values of the total load, respectively.

C. Proportion of Off-Peak Electricity

The proportion of off-peak electricity quantifies the share of total daily load consumption that occurs during off-peak hours, expressed as follows.

$$PLVT = \frac{\sum_{t \in T_{\text{valley}}} P_t \Delta t}{\sum_{t \in T_{\text{day}}} P_t \Delta t} \tag{13}$$

where T_{valley} denotes the off-peak hours, T_{day} represents the 24 h period, and P_t indicates the total load, including both AC loads and charging and discharging loads during time period t.

4.2.2. Constraints of Upper-Level Model

A. Security and Stability Constraints

To meet the requirements for power balance, generation output constraint, transmission line constraint, voltage stability, and overall system security, the following constraints are formulated for the upper-level optimization model.

$$s.t. \begin{cases} \sum\limits_{l=1}^{N_G} P_{\text{gen},l,t} + \sum\limits_{l=1}^{N_{\text{EV}}} P_{\text{EV},l,t} - \sum\limits_{l=1}^{N_L} \left(P_{\text{AC},l,t} + P_{\text{load},l,t} \right) - P_{\text{loss},t} = 0 \\ P_{\text{EV},l} = P_{\text{dis},l} - P_{\text{ch},l} \\ P_{\text{line,min},k} \le P_{\text{line},k} \le P_{\text{line,max},k} \\ U_{i,\min} \le U_i \le U_{i,\max} \end{cases} \tag{14}$$

where $P_{\text{gen},l,t}$ denotes the active power of the l-th generator at time period t; $P_{\text{AC},l,t}$ indicates the AC load of the l-th user at time period t; $P_{\text{load},l,t}$ represents other loads; $P_{\text{EV},l,t}$ signifies the charging and discharging power of the l-th EVs, which can be positive or negative; $P_{\text{ch},l}$ represents the charging power of the l-th EVs; and N_{G}, N_{EV}, and N_{L} denote the number of generators, EVs, and loads, respectively. $P_{\text{loss},t}$ represents the power loss at time period t. $P_{\text{line},k}$ represents the active power flow on transmission line k, constrained by upper and lower capacity limits $P_{\text{line,max},k}$ and $P_{\text{line,min},k}$. U_i denotes the voltage magnitude at node i, bounded within the allowable range $U_{i,\max}$ and $U_{i,\min}$.

B. Incentive Price Mechanism Design Constraints

In accordance with the mechanism design principles outlined in Section 3, the dynamic incentive price model must satisfy the following constraints: price cap, individual rationality, and fairness, formulated as follows.

$$s.t.\begin{cases} p_{\mathrm{dr}} \le p_{\mathrm{dr_max}} \\ u_{\mathrm{g}} \ge 0 \\ u_{\mathrm{A},i} \ge 0, \forall i \in A_{\mathrm{agg}} \\ u_{\mathrm{user},i} \ge 0, \forall i \in A_{\mathrm{user}} \end{cases} \tag{15}$$

where p_{dr} represents the demand response incentive price, bounded above by $p_{\mathrm{dr_max}}$; and A_{agg} and A_{user} denote the sets of aggregators and users, respectively.

4.3. Lower-Level User Optimization Model

4.3.1. Objective Function of Lower-Level Model

The electricity price strategy transmitted by the aggregator to users aims to maximize the joint net benefits of both aggregators and users, thereby achieving optimal coordination between economic incentives and behavioral responses. The corresponding objective function is expressed in the following equation.

$$F_{\mathrm{down}} = \max\left\{ \sum_{i=1}^{N_{\mathrm{agg}}} u_{\mathrm{A},i} + \sum_{i=1}^{N_{\mathrm{user}}} u_{\mathrm{user},i} \right\} \tag{16}$$

where $u_{\mathrm{agg},i}$ and $u_{\mathrm{user},i}$ are detailed in Equations (8) and (11), respectively.

4.3.2. Constraints of Lower-Level Model

A. Power and Price Constraints

Given the operational limitations of V2G infrastructure, and the peak shaving and valley filling objectives, discharging during off-peak hours is prohibited (i.e., the corresponding discharge price is set to zero). Additionally, the discharging and charging power should satisfy the following equations.

$$s.t.\begin{cases} 0 \le P_{\mathrm{dis},t} \le P_{\mathrm{dismax}} \\ 0 \le P_{\mathrm{ch},t} \le P_{\mathrm{chmax}} \\ p_{\mathrm{inc},t} \le p_{\mathrm{dr},t} \\ P_{\mathrm{sh},t} = P_{\mathrm{dis},t} + P_{\mathrm{AC_sh},t} \end{cases} \tag{17}$$

where $P_{\mathrm{dis},t}$ and $P_{\mathrm{ch},t}$ represent the discharge and charge power of the V2G equipment during time period t, respectively; $P_{\mathrm{dis,max}}$ and $P_{\mathrm{ch,max}}$ denote the maximum discharge and charge capacities of the V2G equipment, respectively; $P_{\mathrm{sh},t}$, and $P_{\mathrm{AC_sh},t}$ represent the total peak shaving power and the AC peak shaving power during time period t, respectively.

B. User Response Willingness Constraints

The relationship between the peak shaving power and the incentive price of V2G and AC users plays a key role in value transfer between the upper and lower levels.

For V2G users, participation in discharging is constrained by travel convenience, battery degradation, equipment cost, and incentive prices. According to the consumer psychology model [28,29], when the incentive price exceeds a threshold, the user's responsivity is proportional to the incentive price. This piece-wise linear formulation is widely adopted in user response models due to its computational tractability in large-scale problems and its effectiveness in capturing the aggregate response behavior. Therefore, the discharge responsivity of vehicle users can be characterized as follows.

$$\lambda_{\mathrm{dis}} = \begin{cases} 0 & p_{\mathrm{inc}} \le p_{\mathrm{th_dis}} \\ K_{\mathrm{dis}}(p_{\mathrm{inc}} - p_{\mathrm{th_dis}}) & p_{\mathrm{th_dis}} < p_{\mathrm{inc}} \le p_{\mathrm{s_dis}} \\ \lambda_{\mathrm{max_dis}} & p_{\mathrm{inc}} > p_{\mathrm{s_dis}} \end{cases} \tag{18}$$

where $p_{\text{th_dis}}$ is the just noticeable difference (JND) for vehicle users, $p_{\text{s_dis}}$ is the electricity price saturation threshold, $\lambda_{\text{max_dis}}$ represents the upper limit of the vehicle users' load shifting ratio, and K_{dis} is the slope of the linear region of the V2G piecewise linear function.

The relationship between the responsivity and the response energy is given by Equation (19).

$$\lambda_{\text{dis}} = \frac{E_{\text{d}}}{E_{\text{c}}} \tag{19}$$

$$\begin{cases} E_{\text{d}} = \int_{t_0}^{t} P_{\text{dis},\tau} d\tau \\ E_{\text{c}} = \int_{t_0}^{t} P_{\text{ch},\tau} d\tau \end{cases} \tag{20}$$

where E_{c} and E_{d} represent the charging electricity before coordination and the discharging electricity after coordination during peak hours, respectively, representing the time integral of charging/discharging power. To resolve the potential circular dependency in Equation (19), an iterative method is employed (see Figure 6). The process starts with initializing the incentive price p_{inc}, then determines λ_{dis} and E_{d} through the user response model, and iteratively solves the bi-level model until the incentive price converges.

For vehicle owners, the JND should exceed the incremental cost of V2G discharging. This comprises both direct costs (e.g., battery degradation cost) and indirect costs (e.g., loss of travel convenience, which is zero when the vehicle is not dispatched. Thus, the JND satisfies the following equation.

$$p_{\text{th_dis}} \geq C_{\text{loss}} \tag{21}$$

where C_{loss} represents the equivalent per-kWh battery degradation cost.

The equivalent per-kWh battery degradation cost is derived from the per-kWh depreciation cost of the battery, which depends on the number of discharge cycles [30], satisfying the following equation.

$$C_{\text{loss}} = \frac{C_{\text{b}}}{N_0} \tag{22}$$

where N_0 represents the battery cycle life, and C_{b} represents the battery cost per unit capacity.

This simplified linear model is justified by the operational conditions assumed in this study: (1) the limited discharge duration and low discharge power in destination scenarios constrain the depth of discharge (DoD) to below 60%; (2) the C-rate is maintained below 0.5 C; and (3) the temperature is assumed to remain within the optimal operating range. Under these constraints, a linear degradation approximation provides a reasonable balance between model fidelity and computational tractability for coordination analysis [31,32].

For AC users, the relationship between the responsivity and incentive price similarly satisfies the following equation. It is noteworthy that this formulation employs a lumped-parameter model, which provides a computationally efficient representation of aggregate AC load behavior for coordination studies, effectively balancing model fidelity with tractability.

$$\lambda_{\text{AC}} = \frac{E_{\text{a}} - E_{\text{b}}}{E_{\text{b}}} \tag{23}$$

where E_{a} and E_{b} represent the electricity consumption during the peak hours before and after executing the coordination mechanism, respectively.

The relationship between the AC responsivity and incentive price is calculated using Equation (24).

$$\lambda_{AC} = \begin{cases} 0 & p_{inc} \le p_{th_AC} \\ K_{AC}(p_{inc} - p_{th_AC}) & p_{th_AC} < p_{inc} \le p_{s_AC} \\ \lambda_{max_AC} & p_{inc} > p_{s_AC} \end{cases} \quad (24)$$

where p_{th_AC} is the JND for AC users, p_{s_AC} is the saturation value of the electricity price, λ_{max_AC} represents the maximum achievable load-shaving ratio of the AC load, and K_{AC} is the slope of the linear region of the AC load piecewise linear function.

C. EV Charging and Discharging Constraints

To ensure state of health and travel demand, the state of charge (SOC) during charging and discharging operations is constrained within specified upper and lower bounds, as expressed below.

$$\begin{cases} SOC_{EV,t} = SOC_{EV,0} + \dfrac{1}{E_{EV}}\left(\eta_{ch}\displaystyle\int_{t_0}^{t} P_{ch,\tau}d\tau - \dfrac{1}{\eta_{dis}}\displaystyle\int_{t_0}^{t} P_{dis,\tau}d\tau\right) \\ SOC_{EV,min} \le SOC_{EV,t} \le SOC_{EV,max} \end{cases} \quad (25)$$

where $SOC_{EV,t}$ and $SOC_{EV,0}$ denote the battery SOC at time t and at the initial charging time t_0, respectively; $E_{EV,t}$ represents the rated battery capacity of the electric vehicle; $SOC_{EV,max}$ and $SOC_{EV,min}$ refer to the upper and lower SOC limits; and η_{ch} and η_{dis} indicate the charging and discharging efficiencies. The lower SOC limit is set to retain sufficient energy to meet the user's next travel demand.

5. Experimental Validation and Discussion

5.1. Parameter Settings

To verify the effectiveness of the proposed bi-level optimization model, the IEEE 14-bus system is adopted for analysis, as shown in Figure 7. In this figure, the arrows and numbers represent electrical loads and bus numbers, respectively. Among them, the AC loads and EVs are evenly distributed at Node 2 and Node 3.

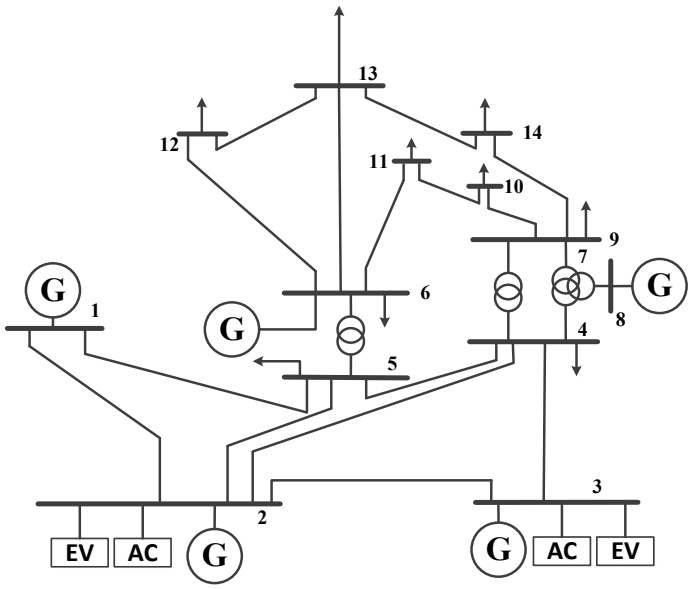


Figure 7. IEEE 14-bus system model diagram.

A typical summer day in a selected region serves as the simulation scenario, with the temporal distributions of AC load and charging/discharging load illustrated in Figures 1 and 2, respectively. Based on historical user behavior data and a survey, the

key parameters for the typical summer day are summarized in Table 2. These parameters include time-of-use electricity prices for AC and EVs, upper limits of demand response incentives, aggregator investment costs, and user response behavior parameters.

Table 2. Parameter Settings.

Stakeholders	Parameter	Value	Parameter	Value
Grid Companies	Off-peak Hours	[0:00,6:00]∪[22:00,24:00]	Peak hours	[8:00,12:00]∪[14:00,15:00]∪[18:00,21:00]
	Flat Hours	[6:00,8:00]∪[15:00,18:00]∪[21:00,22:00]	Critical peak hours	[12:00,14:00]
	Time-of-Use Electricity Price (CNY/kWh)	{critical peak, peak, flat, off-peak} = {1.45, 1.17, 0.68, 0.32}	p_{dr_max}	1.5 CNY/kWh
	Peak AC Load	20.15 million kW	*IRR*	8%
	Peak Charging Load	1.5 million kW	/	/
Aggregators	V2G Investment Cost	700 CNY/kW	V2G O&M cost	35 CNY/kW
	V2G Service Life	8 years	V2G Installed Capacity	2.8 million kW
Users	K_{dis}	[0.2,1.5]	Charging and Discharging Loss	20%
	C_b	600 CNY/kWh	N_0	3500
	K_{AC}	[0.05,0.1]	pth$_{_AC}$	0
	λ_{max_dis}	Vehicle Parking Percentage	λ_{max_AC}	0.2
	Number of AC Users	42.5 million	Number of V2G Users	600 k private users, 200 k office users
	SOC_{min}	60%	SOC_{max}	100%

On the grid side, the demand response program is activated when the total load reaches 85% of the peak value. The corresponding demand response period runs from 09:45 to 17:15, aiming to reduce the peak AC load by approximately 15% to maintain system reliability and supply adequacy.

For aggregators, the primary costs stem from the investment and O&M expenditures of V2G infrastructure. To ensure economic feasibility, the revenue from participating in demand response must be sufficient to offset these costs while maintaining a reasonable profit margin.

For AC and V2G users, the relationship between incentive prices and responsivity, along with the boundary regions, is derived based on the empirical user behavior parameters of both types of users, as depicted in Figure 8. Notably, the upper limit of the V2G responsivity is not constant but is constrained by the time-varying vehicle parking percentage, which does not exceed 1. This relationship is detailed in Figure 3. Assuming that the user response behavior parameters follow a uniform distribution, Monte Carlo random sampling is employed to simulate the response characteristics of AC and V2G users. Considering thermal comfort constraints for AC users, the maximum responsivity is limited to 20%.

5.2. Analysis of the Proposed Coordination Mechanism

To validate the effectiveness of the proposed coordination mechanism, three simulation scenarios are designed for comparative analysis. The objective is to assess system performance from multiple perspectives, including individual rationality, coordination optimization, and overall economic efficiency. The scenarios are configured below.

Scenario 1 (Baseline Scenario): Only thermal generation units are invested in, without implementing any load regulation strategies. In this case, conventional generation units are dispatched to meet load demand. This scenario serves as a benchmark for evaluating the economic efficiency and system performance of traditional capacity expansion approaches relative to the proposed coordination mechanism in shaving peak loads.

Scenario 2: The proposed bi-level game model is employed, but only regulates AC loads. In this scenario, demand-side management strategies are implemented to adjust AC loads, evaluating the effectiveness of single-type flexible load regulation on system peak shaving and its impact on user comfort.

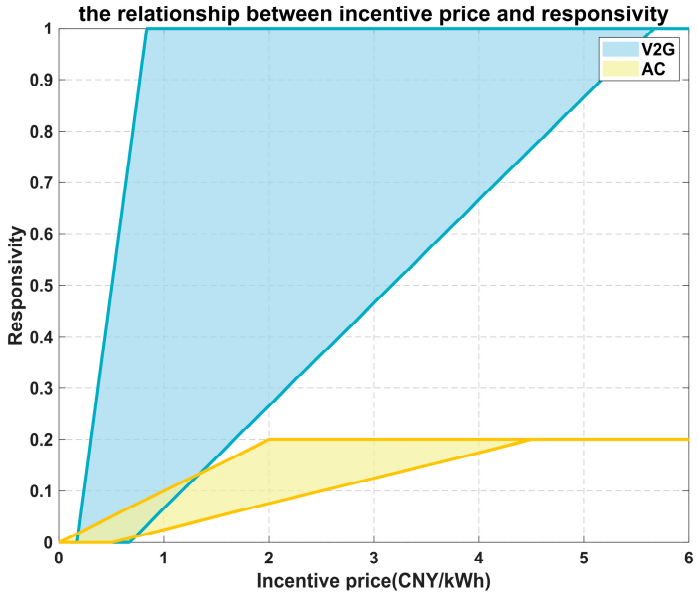


Figure 8. Relationship Between Incentive Prices and User Responsivity.

Scenario 3: The proposed coordination mechanism is implemented, enabling synergistic regulation of both AC and V2G loads. This scenario leverages the proposed optimization model to achieve coordination between AC and charging/discharging loads, examining its comprehensive impacts on system flexibility enhancement, peak loads reduction, stakeholder profitability, and users' response willingness.

5.2.1. Grid Regulation Capability

Based on the bi-level optimization model and parameters established in Section 4, the demand response incentive price curves for Scenarios 2 and 3, along with the corresponding AC and charging/discharging load curves, are depicted in Figures 9 and 10, respectively. As shown in Figures 9 and 10, the system regulation performance under the three scenarios is compared in terms of peak-to-valley ratio and off-peak electricity consumption.

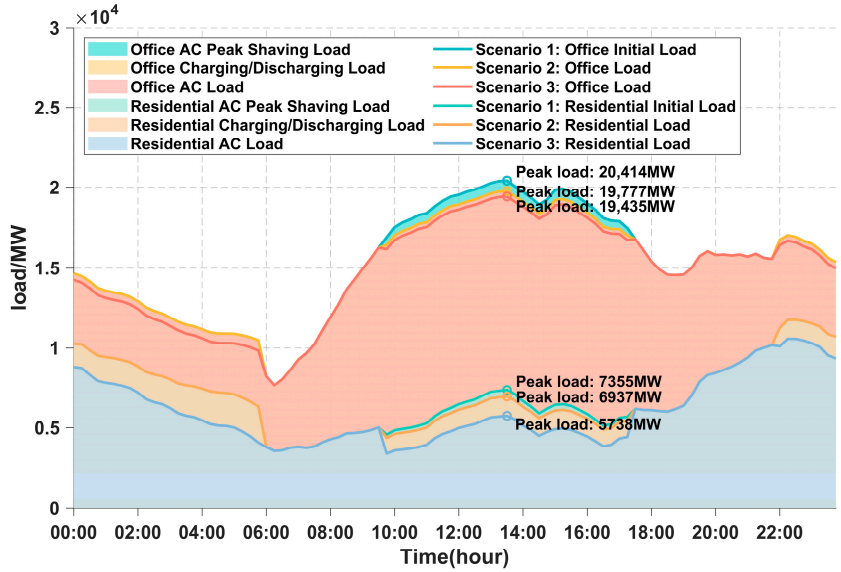


Figure 9. Load Comparison for the Three Scenarios.

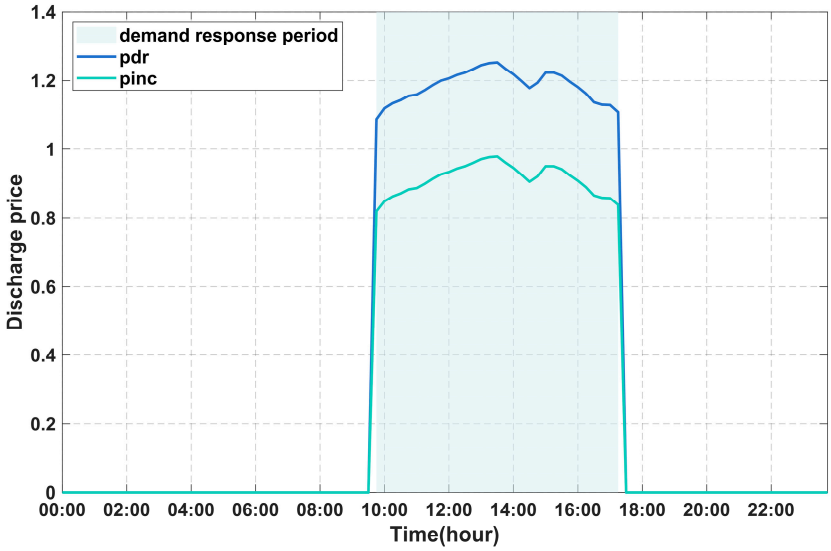


Figure 10. Incentive Price Curve for Bi-level Optimization Model-based Demand Response.

In Scenario 1, where no demand-side control measures are implemented, the superimposed AC and charging loads yield a peak load of 20,410 MW and a valley load of 7610 MW. The peak-to-valley ratio is 2.68, and the proportion of off-peak electricity is 25.4%.

In Scenario 2, applying demand response to AC loads only reduces the total AC load by 1055 MW (comprising 637 MW in office areas, accounting for 5.1% of the regional AC load of 12,480 MW, and 418 MW in residential areas, accounting for 5.3% of the regional AC load of 79,200 MW). Consequently, the peak-to-valley ratio decreases to 2.55, representing a 5% reduction compared with Scenario 1. Due to reduced electricity consumption during peak hours, the proportion of off-peak electricity increases to 26%.

In Scenario 3, under the coordination mechanism, V2G discharging power reaches 1541 MW (including 342 MW in office areas and 1199 MW in residential areas), while AC loads are reduced by 1055 MW. This yields a total peak load reduction of approximately 13%, and lowers the peak-to-valley ratio to 2.32, corresponding to a 13% reduction compared to Scenario 1. By shifting some discharge energy to charging during off-peak hours, the proportion of off-peak electricity increases to 30.4%, marking a 20% improvement compared to Scenario 1. These results demonstrate that price-guided coordination between AC and V2G loads can effectively exploit the flexible demand potential, achieving simultaneous peak shaving and valley filling. The coordination mechanism significantly reduces system peak load and the peak-to-valley ratio, while increasing the proportion of off-peak electricity.

Furthermore, from a spatial distribution perspective, during daytime peak hours, residential AC load is lower than that of office areas, yielding a smaller adjustable potential despite similar relative reduction percentages. In terms of V2G resources, the total V2G resource in residential areas exceeds that of office areas, providing greater adjustable capacity during peak hours.

5.2.2. Economic and Behavioral Analysis

The utility functions for the grid company, aggregators, and users are presented in Figure 11. As shown in Figure 11, the economic outcomes for each stakeholder differ substantially across the three scenarios. In Scenario 1, which relies on investing in generation units to secure power supply, no avoidable costs are generated; thus, the utilities for the grid company, aggregators, and users are essentially zero.

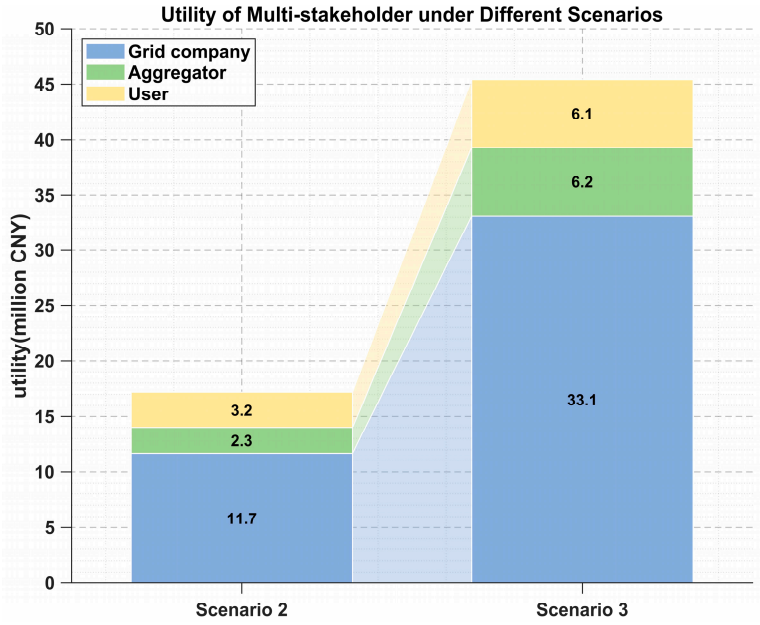


Figure 11. Utilities of the Grid Company, Aggregators, and Users.

In Scenario 2, where AC users participate in demand response, net benefits of approximately 2.3 billion CNY and 3.2 billion CNY are brought to AC aggregators and users, respectively. These benefits primarily originate from the incentive payments for load reduction. The peak-shaving benefit is equivalent to deferring roughly 17.3 billion CNY in generation units and networks investment, achieving a total social welfare of 17.2 billion CNY. This confirms that single-type load participation can yield meaningful yet limited welfare improvements.

In Scenario 3, with both AC and V2G users participating in coordination, the aggregator and user net benefits increase markedly to 6.2 billion CNY and 6.1 billion CNY, respectively. The remarkable growth results from the synergistic effect of coordinated resources, which unlocks greater peak-shaving capacity and creates additional V2G revenue. The peak-shaving benefit is equivalent to reducing grid investment costs by approximately 45.9 billion CNY, providing a total social welfare of 45.4 billion CNY. Overall, the closed-loop value transfer among the grid, aggregators, and users demonstrates significant mutual economic benefits, ensuring the sustainable and self-reinforcing operation of the coordination mechanism.

From the perspective of user experience, the response willingness of AC and V2G users is illustrated in Figure 12. Figure 12 reveals distinct heterogeneity between AC and V2G users. AC users' participation in demand response entails a sacrifice in thermal comfort; therefore, their response willingness rarely reaches 100%. In contrast, V2G users are primarily constrained by battery degradation costs; when the revenue offsets these costs, their response willingness can reach full participation. Under the given incentive prices, the average response rates of AC and V2G users during the demand response period are 13–16% and 75–85%, respectively.

These findings indicate that V2G users have certain advantages over AC users in terms of user experience and response willingness. The proposed coordination mechanism can effectively identify and utilize the heterogeneous response characteristics, thereby precisely unleashing their adjustable potential. Furthermore, the average responsivity in residential and office areas is constrained by time-varying parking availability, confirming the model's capability to capture spatial and behavioral diversity under uniform price signals.

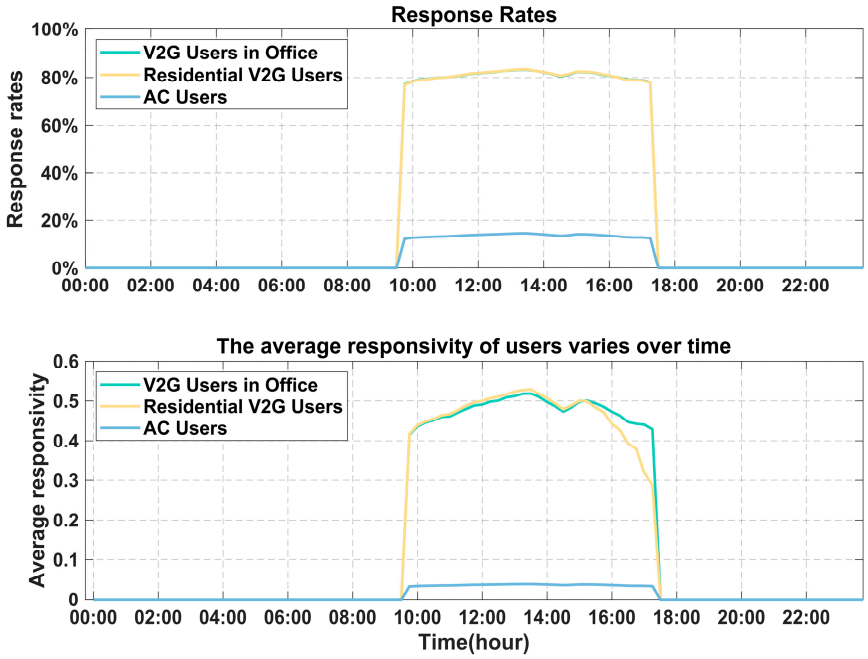


Figure 12. Response Rates of V2G and AC Users.

5.2.3. Spatiotemporal Coupling Evaluation

To validate the effectiveness of the proposed coordination mechanism in mitigating the peak-on-peak phenomenon, the spatiotemporal coupling evaluation indicators in Section 2.2 are employed. Considering that the spatiotemporal coupling of travel remains unchanged, only the spatiotemporal coupling between charging loads and AC loads in Scenario 3 is evaluated. The spatiotemporal coupling heatmap of user charging in residential and office areas is shown in Figure 13.

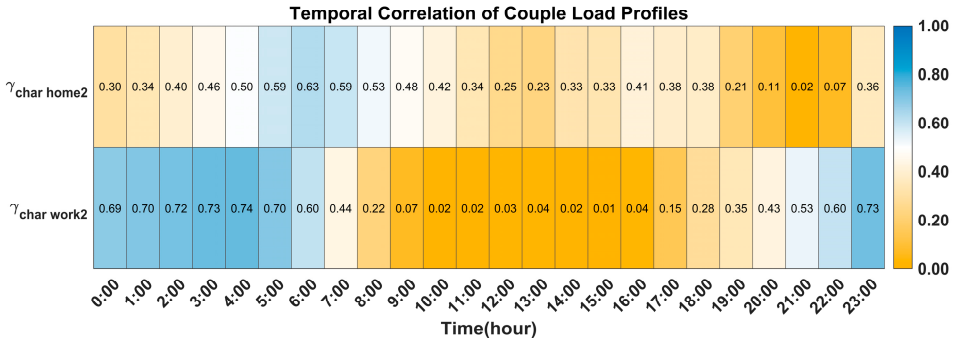


Figure 13. Spatiotemporal Coupling Heatmap of User Charging in Residential-Office Areas under Scenario 3.

A comparison between Figures 4 and 13 reveals a substantial reduction in spatiotemporal coupling following the implementation of the coordination mechanism. Specifically, in residential areas, the value of γ_{ch} during the nighttime hours (22:00–24:00) decreases from above 0.6 to below 0.1. Similarly, in office areas, during weekday morning hours (08:00–10:00), the value drops from above 0.6 to below 0.4. These results indicate that the proposed coordination mechanism effectively alleviates the peak-on-peak problem caused by the superposition of regional AC load and charging load.

6. Conclusions

Against the backdrop of the dual carbon goals, power systems are confronted with rising electricity demand coupled with inefficient and high-cost peak-shaving methods.

Traditional solutions, whether relying on single-type load regulation or generation-side expansion, struggle to mitigate the growing peak-to-valley difference amid economic and environmental constraints. To address this limitation, this study proposes a price-guided coordination mechanism that effectively mobilizes demand-side flexibility, thereby achieving cost-efficient peak load regulation. The main contributions and findings are summarized as follows.

(1) The necessity and feasibility of coordination between V2G and AC loads were systematically demonstrated. Both exhibit highly overlapping spatiotemporal distributions in destination-based scenarios such as commercial buildings, campuses, and residential communities. The advantages of V2G, including small coverage, substantial adjustable potential, and low marginal regulation costs, provide a techno-economic foundation for coordination with AC loads.

(2) A value transfer framework and a bi-level optimization model are developed to achieve multi-stakeholder win-win outcomes. A dynamic incentive-driven closed-loop value transfer mechanism is proposed, interconnecting the grid company, load aggregators, and end-users. Based on this framework, a bi-level optimization model is developed to balance stakeholder interests and realize multi-party win–win outcomes. The model integrates behavioral and technical heterogeneity, explicitly considering AC users' thermal comfort preferences and V2G users' battery degradation costs, thereby enhancing the model's realism and practical applicability for practical deployment.

(3) The proposed coordination mechanism demonstrates superior performance in load management through multi-scenario simulations. Specifically, it achieves a 13% reduction in peak load, a 13% decrease in the peak-to-valley ratio, and a 20% increase in off-peak electricity consumption. Furthermore, the mechanism generates a total social welfare of approximately CNY 45.4 billion, while deferring investments in generation and transmission infrastructure and improving aggregator and user profitability, thereby confirming its multi-win effectiveness and strong practical potential.

In summary, the proposed coordination mechanism offers a technically feasible and economically efficient new pathway for enhancing demand-side flexibility and mitigating peak load pressures in power systems. Its demonstrated efficacy in peak shaving and stakeholder benefits are potentially transferable to other networks with similar demand-side flexibility resources. Future research will further focus on incorporating the uncertainty of renewable energy generation, refining heterogeneous behavioral modeling, detailed battery degradation models, and developing multi-timescale coordination strategies to further improve the robustness and scalability of the proposed mechanism.

Author Contributions: Conceptualization, D.W.; methodology, D.Z.; validation, D.Z.; formal analysis, L.L.; investigation, D.W.; resources, D.W.; data curation, D.Z.; writing—original draft preparation, D.Z.; writing—review and editing, L.L.; visualization, D.Z.; supervision, D.W.; project administration, D.W.; funding acquisition, D.W. All authors have read and agreed to the published version of the manuscript.

Funding: This research was funded by Science and Technology Projects of State Grid Corporation of China, grant number 5400-202417205A-1-1-ZN.

Data Availability Statement: The raw data supporting the conclusions of this article will be made available by the authors on request.

Conflicts of Interest: Author Dan Wu was employed by the State Grid Shanghai Municipal Electric Power Company. The remaining authors declare that the research was conducted in the absence of any commercial or financial relationships that could be construed as a potential conflict of interest.

Abbreviations

The following abbreviations are used in this manuscript:

AC	Air Conditioning
V2G	Vehicle-to-Grid
EV	Electric Vehicle
JND	Just Noticeable Difference
O&M	Operation and Maintenance
SOC	State of Charge
DoD	Depth of Discharge
AHP	Analytic Hierarchy Process

References

1. Ross, S.C.; Vuylsteke, G.; Mathieu, J.L. Effects of Load-Based Frequency Regulation on Distribution Network Operation. *IEEE Trans. Power Syst.* **2019**, *34*, 1569–1578. [CrossRef]
2. Waseem, T.M.; Lin, Z.; Ding, Y.; Wen, F.; Liu, S.; Palu, I. Technologies and Practical Implementations of Air-Conditioner Based Demand Response. *J. Mod. Power Syst. Clean Energy* **2021**, *9*, 1395–1413. [CrossRef]
3. Liu, W.; Zhang, X.; Wu, Y.; Feng, S. Economic Analysis of Renewable Energy in the Electricity Marketization Framework: A Case Study in Guangdong, China. *Front. Energy Res.* **2020**, *8*, 98. [CrossRef]
4. Wang, K.; Niu, D.; Yu, M.; Liang, Y.; Yang, X.; Wu, J.; Xu, X. Analysis and Countermeasures of China's Green Electric Power Development. *Sustainability* **2021**, *13*, 708. [CrossRef]
5. Yang, X.; Niu, D.; Chen, M.; Wang, K.; Wang, Q.; Xu, X. An Operation Benefit Analysis and Decision Model of Thermal Power Enterprises in China Against the Background of Large-Scale New Energy Consumption. *Sustainability* **2020**, *12*, 4642. [CrossRef]
6. Flataker, A.; Malmin, O.K.; Hjelkrem, O.A.; Rana, R.; Korpås, M.; Torsæter, B.N. Impact of Home- and Destination Charging on the Geographical and Temporal Distribution of Electric Vehicle Charging Load. In Proceedings of the 18th International Conference on the European Energy Market (EEM), Ljubljana, Slovenia, 13–15 September 2022; pp. 1–6. [CrossRef]
7. Pagany, R.; Marquardt, A.; Zink, R. Electric Charging Demand Location Model—A User- and Destination-Based Locating Approach for Electric Vehicle Charging Stations. *Sustainability* **2019**, *11*, 2301. [CrossRef]
8. Chen, L.; Zhou, J.; Chen, Y.; Cao, Z.; Dong, X.; Choo, K.-K.R. PADP: Efficient Privacy-Preserving Data Aggregation and Dynamic Pricing for Vehicle-to-Grid Networks. *IEEE Internet Things J.* **2021**, *8*, 7863–7873. [CrossRef]
9. Chen, P.; Han, L.; Xin, G.; Zhang, A.; Ren, H.; Wang, F. Game Theory Based Optimal Pricing Strategy for V2G Participating in Demand Response. *IEEE Trans. Ind. Appl.* **2023**, *59*, 4673–4683. [CrossRef]
10. Al-Obaidi, A.A.; Farag, H.E.Z. Optimal Design of V2G Incentives and V2G-Capable Electric Vehicles Parking Lots Considering Cost-Benefit Financial Analysis and User Participation. *IEEE Trans. Sustain. Energy* **2024**, *15*, 454–465. [CrossRef]
11. Liu, Y.; Yu, H.; Wang, F.; Huang, M.; Shi, J.; Liu, W.; Wu, Y.; Li, L.; Liu, M. Electric Vehicle Scheduling Strategy Based on Dynamic Adjustment Mechanism of Time-of-Use Price. *Front. Smart Grids* **2025**, *4*, 1554251. [CrossRef]
12. Wang, Y.; Sun, W. A Two-Stage Robust Pricing Strategy for Electric Vehicle Aggregators Considering Dual Uncertainty in Electricity Demand and Real-Time Electricity Prices. *Sustainability* **2024**, *16*, 3593. [CrossRef]
13. Winzer, C.; Hensler-Ludwig, P. Design and Impact of Grid Tariffs. *Energies* **2024**, *17*, 1364. [CrossRef]
14. Goh, H.H.; Zong, L.; Zhang, D.; Dai, W.; Lim, C.S.; Kurniawan, T.A.; Goh, K.C. Orderly Charging Strategy Based on Optimal Time of Use Price Demand Response of Electric Vehicles in Distribution Network. *Energies* **2022**, *15*, 1869. [CrossRef]
15. Das, R.; Wang, Y.; Putrus, G.; Kotter, R.; Marzband, M.; Herteleer, B.; Warmerdam, J. Multi-Objective Techno-Economic-Environmental Optimisation of Electric Vehicle for Energy Services. *Appl. Energy* **2020**, *257*, 113965. [CrossRef]
16. Yu, S.H.; Du, Z.B.; Chen, L.D. Optimal Regulation Strategy of Electric Vehicle Charging and Discharging Based on Dynamic Regional Dispatching Price. *Front. Energy Res.* **2022**, *10*, 873262. [CrossRef]
17. Bakhuis, J.; Barbour, N.; Molin, E.; Chappin, É.J.L. Understanding User Preferences Regarding Vehicle-to-Grid (V2G): A Latent Class Choice Analysis. *Transp. Res. Part A Policy Pract.* **2025**, *199*, 104610. [CrossRef]
18. Zhang, C.; Kitamura, H.; Goto, M. Exploring V2G Potential in Tokyo: The Impact of User Behavior Through Multi-Agent Simulation. *IEEE Access* **2024**, *12*, 118981–119002. [CrossRef]
19. Chen, C.-F.; Xu, X.; Cao, Z.; Mockus, A.; Shi, Q. Analysis of Social–Psychological Factors and Financial Incentives in Demand Response and Residential Energy Behavior. *Front. Energy Res.* **2023**, *11*, 932134. [CrossRef]
20. Maheshwari, A.; Paterakis, N.G.; Santarelli, M.; Gibescu, M. Optimizing the Operation of Energy Storage Using a Non-Linear Lithium-Ion Battery Degradation Model. *Appl. Energy* **2020**, *261*, 114360. [CrossRef]

21. Krueger, H.; Cruden, A. Integration of Electric Vehicle User Charging Preferences into Vehicle-to-Grid Aggregator Controls. *Energy Rep.* **2020**, *6*, 86–95. [CrossRef]
22. Bao, Y.; Chang, F.; Shi, J.; Yin, P.; Zhang, W.; Gao, D.W. An Approach for Pricing of Charging Service Fees in an Electric Vehicle Public Charging Station Based on Prospect Theory. *Energies* **2022**, *15*, 5308. [CrossRef]
23. Lesieutre, B.; Bravo, R.; Yinger, R.; Chassin, D.; Huang, H.; Lu, N.; Hiskens, I.; Venkataramanan, G. *Load Modeling Transmission Research. Final Project Report*; Report No. LBNL-5677E; Lawrence Berkeley National Laboratory (LBNL): Berkeley, CA, USA, 2012.
24. Liu, Y.; Eyre, N.; Darby, S. *Follow-Up Analysis of DR Potential of Commercial Buildings for Summer and Winter in Shanghai*; Natural Resources Defense Council: Beijing, China, 2016.
25. Zhang, Z.; Chen, Z.; Gümrükcü, E.; Xing, Q.; Ponci, F.; Monti, A. A Nudge-Based Approach for Day-Ahead Optimal Scheduling of Destination Charging Station with Flexible Regulation Capacity. *IEEE Trans. Transp. Electrif.* **2024**, *10*, 8498–8512. [CrossRef]
26. Lauss, L.; Meier, A.; Auer, T. Uncertainty and Sensitivity Analyses of Operational Errors in Air Handling Units and Unexpected User Behavior for Energy Efficiency and Thermal Comfort. *Energy Effic.* **2022**, *15*, 4. [CrossRef]
27. Fritsch, J.; Poudineh, R. Gas-to-Power Market and Investment Incentive for Enhancing Generation Capacity: An Analysis of Ghana's Electricity Sector. *Energy Policy* **2016**, *92*, 92–101. [CrossRef]
28. Wu, H.; Wang, J.; Ren, Y.; Bi, R.; Sun, M.; Wei, W. Response Reliability and Risk Analysis of Users under Time-of-use Price. *IET Gener. Transm. Distrib.* **2021**, *16*, 839–850. [CrossRef]
29. Xu, X.; Li, K.; Wang, F.; Mi, Z.; Jia, Y.; Wei, W.; Jing, Y. Evaluating Multitimescale Response Capability of EV Aggregator Considering Users' Willingness. *IEEE Trans. Ind. Appl.* **2021**, *57*, 3366–3376. [CrossRef]
30. Wang, D.; Coignard, J.; Zeng, T.; Zhang, C.; Saxena, S. Quantifying Electric Vehicle Battery Degradation from Driving vs. Vehicle-to-Grid Services. *J. Power Sources* **2016**, *332*, 193–203. [CrossRef]
31. Zhao, Y.; Yuan, Q.; Yang, L.; Liang, G.; Cheng, Y.; Wu, L.; Lin, C.; Che, R. Zero-Strain $NiNb_2O_6$ Fibers for All-Climate Lithium Storage. *Nano-Micro Lett.* **2024**, *17*, 15. [CrossRef]
32. Made, R.I.; Lin, J.; Zhang, J.; Zhang, Y.; Moh, L.C.; Liu, Z.; Ding, N.; Chiam, S.Y.; Khoo, E.; Yin, X.; et al. Health Diagnosis and Recuperation of Aged Li-Ion Batteries with Data Analytics and Equivalent Circuit Modeling. *iScience* **2024**, *27*, 109416. [CrossRef]

Disclaimer/Publisher's Note: The statements, opinions and data contained in all publications are solely those of the individual author(s) and contributor(s) and not of MDPI and/or the editor(s). MDPI and/or the editor(s) disclaim responsibility for any injury to people or property resulting from any ideas, methods, instructions or products referred to in the content.